0013-7227/05/$15.00/0
Printed in U.S.A.

Endocrinology 146(2):728–735

doi: 10.1210/en.2004-1021

Hydrogen Peroxide Is Essential for Estrogen-Deficiency Bone Loss and Osteoclast Formation

Jenny M. Lean, Chris J. Jagger, Barrie Kirstein, Karen Fuller, and Timothy J. Chambers

Department of Cellular Pathology, St. George's Hospital Medical School, London SW17 0RE, United Kingdom

We recently found that estrogen deficiency leads to a lowering of thiol antioxidant defenses in rodent bone. Moreover, administration of agents that increase the concentration in bone of glutathione, the main intracellular antioxidant, prevented estrogen-deficiency bone loss, whereas depletion of glutathione by buthionine sulfoximine administration provoked substantial bone loss. To analyze further the mechanism by which antioxidant defenses modulate bone loss, we have now compared expression of the known antioxidant enzymes in osteoclasts. We found that glutathione peroxidase 1 (Gpx), the enzyme primarily responsible for the intracellular degradation of hydrogen peroxide, is overwhelmingly the predominant antioxidant enzyme expressed by osteoclasts and that its expression was increased in bone marrow macrophages by receptor activator of nuclear factor-κB ligand (RANKL) and in osteoclasts by 17β-estradiol. We therefore tested the effect of overexpression of Gpx in osteoclasts by stable transfection of RAW 264.7 (RAW) cells, which are capable of osteoclastic differentiation in response to RANKL, with a Gpx-expression construct. Osteoclast formation was abolished. The Gpx expression construct also suppressed RANKL-induced nuclear factor-κB activation and increased resistance to oxidation of dihydrodichlorofluorescein by exogenous hydrogen peroxide. We therefore tested the role of hydrogen peroxide in the loss of bone caused by estrogen deficiency by administering pegylated catalase to mice. We found that catalase prevented ovariectomy-induced bone loss. These results suggest that hydrogen peroxide is the reactive oxygen species responsible for signaling the bone loss of estrogen deficiency. (*Endocrinology* 146: 728–735, 2005)

BONE RESORPTION IS essential for calcium homeostasis and the modeling and remodeling of bone. However, excessive resorption is the cause of bone loss observed in common diseases such as postmenopausal osteoporosis, rheumatoid arthritis, and periodontitis and is responsible for the destruction of bone that occurs around skeletal metastases and in Paget's disease of bone.

The cell responsible for bone resorption is the osteoclast. It is derived from cells of the mononuclear phagocyte system, which are induced to osteoclastic differentiation and function through the actions of macrophage colony-stimulating factor (M-CSF) and receptor activator of nuclear factor-κB ligand (RANKL), cytokines that are expressed physiologically by cells of the osteoblastic lineage (see Refs. 1–3).

Several of the intracellular signals essential for osteoclast formation, including nuclear factor-κB (NFκB), c-Jun amino-terminal kinase, phosphatidylinositol 3-kinase, and p38 MAPK, are sensitive to reactive oxygen species (ROS) (4), and it has become clear that osteoclastic differentiation and function are stimulated by ROS (5–7). Moreover, osteoclasts contain a nicotinamide adenine dinucleotide phosphate reduced (NADPH) oxidase (8), an enzyme that is capable of cytokine-induced generation of ROS. Recently we found evidence that estrogen deficiency causes osteoclastic hyperresorption by lowering antioxidant defenses in osteoclastic cells, thus entraining a ROS-mediated increase in osteoclastic differentiation and function (7). We also found that systemic administration of the antioxidants ascorbate or *N*-acetyl cysteine prevented the loss of bone that normally occurs in mice rendered estrogen deficient by ovariectomy and that buthionine sulfoximine, which depletes tissues of glutathione, the major cellular antioxidant, caused bone loss. Osteoclast formation has been shown to depend on NFκB activation (9, 10). NFκB is a known target for activation by ROS (11–13), and we found that oxidants induced, and estrogen and antioxidants suppressed, activation in osteoclasts of NFκB.

The central role of ROS in bone loss caused by estrogen deficiency led us to characterize the antioxidant defense system of osteoclasts. We found that glutathione peroxidase 1 (Gpx) was the predominantly expressed antioxidant enzyme and that its expression in osteoclasts was increased by RANKL and 17β-estradiol. We therefore tested the effect of Gpx overexpression by transfection of RAW 264.7 (RAW) cells with a plasmid that coded for expression of Gpx. We found that Gpx overexpression abrogated osteoclast formation, suggesting a role for Gpx and hydrogen peroxide in the modulation of osteoclastic differentiation. We then went on to test the role of hydrogen peroxide *in vivo* by administering mice-pegylated catalase (CAT) and found that CAT prevented bone loss after ovariectomy. These results suggest that estrogen deficiency causes bone loss by lowering the content of Gpx in osteoclasts, so enabling an increase in hydrogen peroxide, which leads to increased osteoclasts.

First Published Online November 4, 2004

Abbreviations: CAT, Catalase; DCFH-DA, dihydrodichlorofluorescein diacetate; EMEM, MEM with Earle's salts; FCS, fetal calf serum; Gpx, glutathione peroxidase 1; M-CSF, macrophage colony-stimulating factor; NADPH, nicotinamide adenine dinucleotide phosphate reduced; NFκB, nuclear factor-κB; RANKL, receptor activator of NF-κB ligand; RAW, RAW 264.7; ROS, reactive oxygen species; TRAP, tartrate-resistant acid phosphatase.

***Endocrinology* is published monthly by The Endocrine Society (http://www.endo-society.org), the foremost professional society serving the endocrine community.**

Materials and Methods

Media and reagents

Nonadherent, M-CSF-dependent bone marrow cells were incubated with MEM with Earle's salts (EMEM) (Sigma, Poole, Dorset, UK), supplemented with 10% fetal calf serum (FCS) (Autogen Bioclear, Calne, Wiltshire, UK). RAW cells were maintained in DMEM (Sigma) with 10% FCS. All media were supplemented with 2 mM glutamine, 100 IU/ml benzylpenicillin, and 100 μg/ml streptomycin (Sigma). Incubations were performed at 37 C in 5% CO_2 in humidified air. Recombinant human M-CSF was provided by Chiron Corp. (Emeryville, CA); soluble recombinant human RANKL and recombinant murine TNFα were purchased from Insight Biotechnology Ltd. (Wembley, Middlesex, UK). 17β-Estradiol and 17α-estradiol were from Sigma, and ICI 182,780 was from Tocris Cookson Ltd. (Avonmouth, Bristol, UK).

Isolation and culture of bone marrow cells

Bone marrow cells were isolated from male MF1 mice and cultured as previously described (14). Briefly, 5- to 8-wk-old mice were killed by cervical dislocation. Femora and tibiae were aseptically removed and dissected free of soft tissue. The bone ends were cut, and the marrow was flushed out into a petri dish by slowly injecting PBS at one end of the bone using a sterile 21-gauge needle. The bone marrow suspension was carefully agitated through a 21-gauge needle to obtain a single cell suspension. Bone marrow cells were then washed, resuspended in EMEM/FCS, and incubated at a density of 3×10^5 cells/ml for 24 h in a 75-cm^2 flask (Greiner, Stonehouse, Gloucester, UK) with M-CSF (5 ng/ml) to deplete cell preparations of stroma. After 24 h, nonadherent cells were harvested, washed, and resuspended in EMEM/FCS for subsequent incubation.

Real-time PCR analysis of gene expression in bone marrow-derived osteoclasts

Next, 9×10^6 M-CSF-dependent nonadherent bone marrow precursors were added to 75 cm^2 tissue culture flasks and cells incubated for 5 d in the presence of M-CSF or M-CSF (50 ng/ml) and RANKL (50 ng/ml). Cultures were fed every 2–3 d and 2 h before harvesting RNA. After incubation, cultures were washed to remove nonadherent cells and total RNA harvested using RNeasy minikits (Qiagen, Crawley, Sussex, UK). Four micrograms total RNA were reverse transcribed for 1 h at 42 C using 200 pmol of random hexamers (Amersham Biosciences, Amersham, Bucks, UK), 50 μmol deoxynucleotide triphosphates, and 600 U Muloney murine leukemia virus reverse transcriptase (Invitrogen Life Technologies, Paisley, UK) in a 50-μl reaction. This was then diluted to a final volume of 100 μl. Real-time PCR was carried out using the I-Cycler (Bio-Rad Laboratories, Hemel Hempstead, Herts, UK) using SYBR Green for detection of PCR products. Two microliters of either external plasmid standards or a cDNA was added to a final reaction volume of 25 μl containing 200 μM primers, 200 μM deoxynucleotide triphosphates, 3 mM $MgCl_2$, 0.625 U platinum Taq polymerase, 0.25 U AmpErase UNG, and 2.5 μl 10 $\times$ SYBR Green PCR buffer (universal PCR master mix; Applied Biosystems, Warrington, Chesire, UK). Standard curves were generated using plasmid clones containing the corresponding cDNA (see Table 1 for primers, product lengths, and accession numbers). The linear range of the assay was determined by the amplification of log serial dilutions of plasmids from 500 to 5×10^6. Copy number relative to β-actin (15) copy number in the same sample was calculated for each sample. At the end of the PCR run, a melt-curve analysis was performed to ensure product specificity.

Effect of RANKL and 17β-estradiol on bone marrow macrophages and osteoclasts

M-CSF-dependent nonadherent bone marrow precursors were added to 75-cm^2 tissue culture flasks and cells incubated for 5 d in the presence of M-CSF (50 ng/ml) or M-CSF and RANKL (50 ng/ml). After 5 d, the cells were washed and medium replaced with phenol red-free EMEM with charcoal-stripped serum (7) with or without 17β-estradiol (10^{-9} M) for 24 h. RNA was isolated as above, reverse transcribed, and real-time PCR performed. Gpx1 was analyzed in the four groups and levels corrected for β-actin copy number.

Similarly, bone marrow-derived osteoclasts (bone marrow precursors grown in M-CSF and RANKL as above for 5 d) were incubated in ICI 182,780 (10^{-7} M) and 17α-estradiol (10^{-9} M) in phenol red-free EMEM with charcoal-stripped serum for 24 h. For Northern analysis, 10 μg total RNA were size separated in a 1.2% agarose gel, blotted, and hybridized for mouse Gpx1 or β-actin as previously described (16). Probes were labeled with [α-^{32}P]dATP using the Megaprime DNA labeling system (Amersham).

TABLE 1. Primers used for real-time analysis of gene expression in osteoclasts, together with their expected product length and GenBank accession number

	Product length (bp)	Forward primer	Reverse primer	GenBank accession no.
β-Actin	197	GTCATCACTATTGGCAACGAG	CCTGTCAGCAATGCCTGGGTACAT	M12481
Glutathione reductase	245	CTTTCAGCTGGAGGACTTGC	CCAGGCCTGATGATGTCTTT	X76341
Peroxiredoxin 1	184	ACACCCAAGAAACAAGGAGGATT	CAACGGGAAGATCGTTTATTGTTA	NM_011034
Peroxiredoxin 2	180	AACGCGCAAATCGGAAAGT	AGTCCTCAGCATGGTCGCTAA	NM_011563
Peroxiredoxin 3	204	GGCCACATGAACATCACACTGT	CAAACTGGAACGCCTTTACCA	NM_007452
Peroxiredoxin 4	160	TCCTGTTGCGGACCGAAT	GATCTTGGCTTTGCTTAGATGCA	NM_016764
Peroxiredoxin 5	183	GAAAGAAGCAGGTTGGGAGTGT	CCCAGGGACTCCAAACAAAA	NM_012021
Peroxiredoxin 6	260	TTGATGATAAGGGCAGGGAC	CTACCATCACGCTCTCTCCC	NM_007453
Catalase	198	GCGTCCAGTGCGCTGTAGA	TCAGGGTGGACGTCAGTGAA	L25069
Glutathione peroxidase 1	196	GGGACTACACCGAGATGAACGA	ACCATTCACTTCGCACTTCTCA	NM_008160
Glutathione peroxidase 2	160	GAGGAACAACTACCCGGGACTA	ACCCCCAGGTCGGACATACT	NM_030677
Glutathione peroxidase 3	169	GCCAGCTACTGAGGTCTGACAGA	CCACCTGGTCGAACATACTTGAG	NM_008161
Glutathione peroxidase 4	197	TCTGGCAGGCACCATGTGT	CGGGCATGCAGATCGACTA	NM_08162
Thioredoxin 1	190	TTTCCATCTGGTTCTGCTGAGA	TGGAAGAAGGGCTTGATCATTT	NM_011660
Thioredoxin reductase	301	TCCCATGCAGTGGAGAAGAT	GCTGCTCCAACTGTGTCTTG	NM_015762
Glutaredoxin 1	160	CAACACCAGTGCGATTCAAGA	GCAGAGCTCCAATCTGCTTCA	NM_053108
Glutaredoxin 2	205	TGGAATATGGCAACCAGTTTCA	GGCGACTATCCACATCATTCAA	AF380337
Superoxide dismutase 1	150	TGGGTTCCACGTCCATCAGTA	ACCGTCCTTTCCAGCAGTCA	XM_128337
Superoxide dismutase 2	160	ATTAACGCGCAGATCATGCA	TGTCCCCCACCATTGAACTT	NM_0313671
Superoxide dismutase 3	181	CCAGCTTCGACCTAGCAGACA	CAGCGTGGCTGATGGTTGTA	NM_011435
γ-Glutamyl cysteine synthetase (catalytic subunit)	302	AACAAGAAACATCCGGCATC	CGTAGCCTCGGTAAAATGGA	U85414
γ-Glutamyl cysteine synthetase (regulatory subunit)	299	TGGAGCAGCTGTATCAGTGG	CCTTTTGGCTTGCAGAATGT	U95053

Vector construction

The full-length coding sequences for mouse Gpx 1 (NM_008160) was cloned from mouse bone marrow macrophage RNA after reverse transcription using Muloney murine leukemia virus (Invitrogen Life Technologies), using standard procedures. The sequences with a FLAG tag on the antisense primer was amplified using Gpx1 sense, ATG TGT GCT GCT CGG CTC; Gpx antisense, TTA CTT GTC ATC GTC GTC CTT GTA GTC GGA GTT GCC AGA CTG CTG. The resultant amplicon was subcloned into pGEM-Teasy (Promega, Southampton, Hants, UK) and sequenced. Gpx1-FLAG was excised from pGEM-Teasy with *Not*I, subcloned into the *Not*I site of pcDNA3.1(+), and screened for orientation with *Apa*I.

Transfection of RAW cells

The 2×10^5 RAW cells were transfected with 1 μg pcDNA3.1(+) vector DNA, either empty or containing Gpx1-FLAG using FuGene 6 transfection reagent (Roche Diagnostics Ltd., Lewes, East Sussex, UK), according to their instructions. Cells were incubated in serum-free medium containing the Fugene/DNA mix for 6 h. For stable transfectants, cells were incubated in fresh medium containing 10% FCS for 48 h and then selected with 750 μg/ml G418 (Invitrogen Life Technologies). After 10 d, surviving cells were cloned and expanded.

Osteoclast formation by RAW cells expressing Gpx1

The 10^4 RAW cells that had either been stably transfected with empty vector or the Gpx1 expression vector were added to a 96-well plate (Greiner) containing a Thermanox coverslips (Invitrogen Life Technologies) and 200 μl culture medium per well, with or without RANKL (100 ng/ml) or TNFα (100 ng/ml). Cultures were fed every 2–3 d by replacing 120 μl medium with an equal volume of fresh medium and cytokines. Coverslips were assessed for tartrate-resistant acid phosphatase (TRAP) positivity.

TRAP cytochemistry

Osteoclast formation in cultures of transfected RAW cells was evaluated by quantification of TRAP-positive multinuclear cells. After incubation, cells on coverslips were fixed in 10% formalin for 10 min, washed, permeabilized in acetone for 10 min, washed, and stained for acid phosphatase in the presence of 0.05 M sodium tartrate using the Leucognost-AP cytochemical reagent kit (VWR International Ltd., Poole, Dorset, UK). Cells were counterstained with hematoxylin. TRAP-positive cells with three or more nuclei (multinuclear cells) were counted. However, TRAP-positive cells after treatment with TNFα were mononuclear. These were counted.

NFκB p50 nuclear binding and competitor assay

RAW cells stably transfected with either empty vector or Gpx1-expression vector were treated with 50 ng/ml RANKL for 1 h before nuclear extracts were harvested as per manufacture's instruction (BD Biosciences Clontech, Palo Alto, CA). The transfactor colorimetric kit (BD Biosciences Clontech) was used to detect the NFκB p50 nuclear binding from the nuclear extracts. An increase in the OD_{630} correlates to an increase in the NFκB p50 nuclear binding. Twenty micrograms of nuclear extract were used. Two hundred nanograms of competitor Oligo decreases the signal because transcription factor binding is competed away and is used to show specificity of binding activity.

Dihydrodichlorofluorescein diacetate (DCFH-DA) assay

DCFH-DA was used to assess intracellular ROS. This probe diffuses readily into cells. Once inside, the ester groups are hydrolyzed by intracellular esterases, releasing the dichloro derivative. This is oxidized to the fluorescent parent dye by intracellular ROS (17). RAW cells stably transfected with empty vector or the Gpx1 expression vector were seeded at 2×10^5 per well in black 96-well plates. After 24 h cells were washed and treated with 10 μM DCFH-DA for 15 min. Increasing concentrations of H_2O_2 were added for a further 10 min. Cells were washed and read on a fluorescent plate reader in 100 μl PBS (excitation 485 nm/emission 530 nm wavelengths). Cells were then lysed in 0.1% Triton X-100 and the lysate used for protein determination by Coomassie blue method (Coomassie Plus 200, Pierce, Rockford, IL).

Effect of CAT on ovariectomy-induced bone loss

Six- to 8-wk-old female MF1 mice were obtained from Harlan Olac (Oxon, UK). Animals were ovariectomized or sham ovariectomized. Mice were administered pegylated CAT (Sigma) 250 U/animal ip or vehicle (PBS) daily. All animals were pair fed to sham-ovariectomized PBS-control mice and killed after 2 wk. Weights of the mice (grams) before (and after) the experiment ($\pm$ SEM) were as follows: sham/vehicle, 27.7 $\pm$ 0.4 (28.8 $\pm$ 0.5); ovariectomized/vehicle, 27.0 $\pm$ 1.0 (31.2 $\pm$ 0.9); sham/CAT, 27.5 $\pm$ 0.6 (28.4 $\pm$ 0.5); ovariectomized/CAT, 27.8 $\pm$ 0.5 (30.4 $\pm$ 0.5). Success of ovariectomy was confirmed by absence of ovaries and atrophy of uteri. Femora were removed, cleaned of soft tissue, fixed for 24 h in 10% phosphate buffered formalin, demineralized in 10% buffered EDTA for 7 d, dehydrated through graded alcohols, and embedded in paraffin wax. Bones were processed for histomorphometric analysis as described (18). Histomorphometry of the distal femur was performed on cancellous bone at least 0.3 mm beyond the growth plate to exclude any primary spongiosa. For each bone, two fields in each of three sections were measured to include at least 6 cm of bone surface.

Statistical analysis.

Statistical analysis was by ANOVA (Fisher's protected least significant difference test) for multiple comparisons.

Results

Gpx is the predominant antioxidant enzyme expressed by osteoclasts and is up-regulated by 17β-estradiol

We first compared RNA expression of the known antioxidant enzymes in osteoclasts. For this, osteoclasts were derived by incubation of murine M-CSF-dependent nonadherent cells in M-CSF and RANKL for 5 d. Nonadherent cells were washed away and the RNA collected from adherent cells for analysis by real-time PCR. We found that expression of RNA for Gpx exceeded that of any other species by an order of magnitude (Fig. 1).

Gpx was expressed at a higher level in osteoclasts than in bone marrow macrophages (Fig. 2). We also found that Gpx expression was augmented in osteoclasts by 17β-estradiol. This increase was inhibited by the pure antiestrogen ICI 182,780 (Fig. 2). The ability of RANKL and 17β-estradiol, but not the nonreceptor binding stereoisomer 17α-estradiol, to stimulate Gpx expression was confirmed by Northern analysis (Fig. 2). The magnitude of the increase in Gpx expression in osteoclasts by 17β-estradiol is similar to the magnitude of the changes in osteoclastic parameters seen after ovariectomy (see Fig. 6).

Osteoclastic differentiation is abrogated in RAW cells stably transfected with a Gpx expression construct

To assess the role of Gpx in osteoclast formation, RAW cells were transfected with a vector coding for expression of human Gpx, or empty vector. After 2 d cells were selected for stable integrants by addition of G418. Ten days later, surviving cells were cloned and expanded. When stably integrated cells were incubated with RANKL, we found that the osteoclastic differentiation in both of the RAW cell clones transfected with the Gpx expression construct was virtually nonexistent, as judged by the formation of osteoclast-like TRAP-positive multinuclear cells (Fig. 3), compared with the two clones of cells transfected with empty vector. Similar

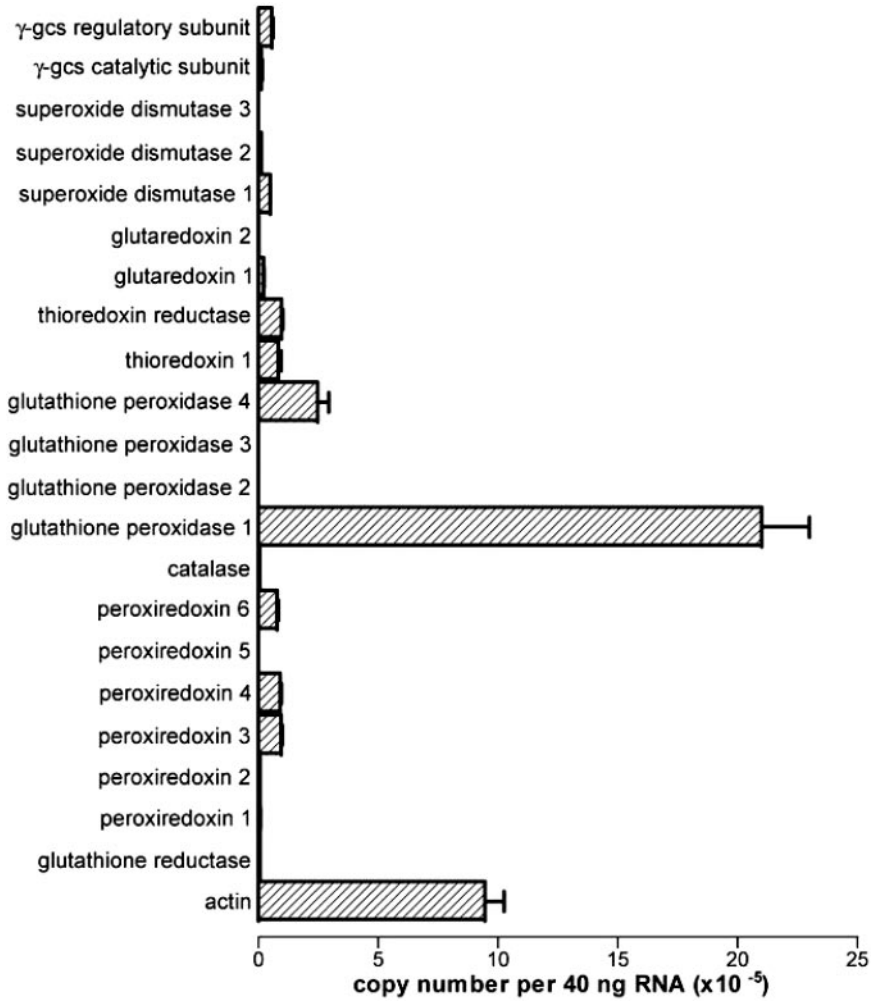

FIG. 1. Real-time PCR assessment of antioxidant gene expression in bone marrow-derived osteoclasts. Murine M-CSF-dependent bone marrow cells incubated in M-CSF (50 ng/ml) and RANKL (30 ng/ml) for 6 d before assessment of gene expression. Results expressed per 40 ng RNA.

virtual abolition of osteoclastic differentiation by the Gpx expression vector was observed in RAW cells incubated with TNFα. Whereas TRAP-positive cells were induced by TNFα in RAW cells stably transfected with empty vector, none were observed in cultures of RAW cells transfected with the Gpx expression construct (Fig. 3).

This virtual abolition of osteoclasts is unlikely to be a toxic effect of the transfected gene because macrophage formation was unaffected: total cell numbers in cultures of RAW cells transfected with Gpx were 29,550 ± 3,450 cells/cm^2 (mean ± SEM) after incubation for 5 d without RANKL, and 2,700 ± 330 after incubation with RANKL, whereas total cell numbers of RAW cells transfected with empty vector were 25,350 ± 2,950 without RANKL and 31,150 ± 1340 after incubation with RANKL. However, although this suggests that Gpx overexpression is not toxic to macrophages, we cannot exclude a toxic effect specifically on osteoclasts or osteoclastic differentiation. We have noted very similar inhibition specifically of osteoclast formation in RAW cells stably transfected with a second antioxidant gene (peroxiredoxin 1) (data not shown), suggesting that this abolition of osteoclasts is due to the antioxidant activity of Gpx.

Stable transfection of RAW cells with Gpx expression vector strongly suppresses NFκB activation and DCF-fluorescence

RANKL has been shown to activate the transcription factor NFκB, activation of which has been shown to be essential for osteoclast formation and activation. It is also known that NFκB activation is augmented by ROS. We therefore compared the ability of RANKL to augment NFκB activity in RAW cells stably transfected with the Gpx expression vector *vs.* RAW cells transfected with empty vector. Stably transfected RAW cells with either empty vector or Gpx were incubated with 50 ng RANKL for 1 h and nuclear extracts harvested. We found that whereas NFκB was strongly activated in empty-RAW cells (Fig. 4), activation was essentially abolished in Gpx-RAW cells. Gpx-RAW cells also showed a substantially greater ability to resist the oxidation of DCF caused by exogenous hydrogen peroxide (Fig. 5). These results suggest that endogenous hydrogen peroxide is required for NFκB activation and osteoclastic differentiation by RANKL.

Administration of pegylated CAT to mice prevents ovariectomy-induced bone loss

The ability of estrogen to increase Gpx expression in osteoclasts and the ability of Gpx overexpression to suppress

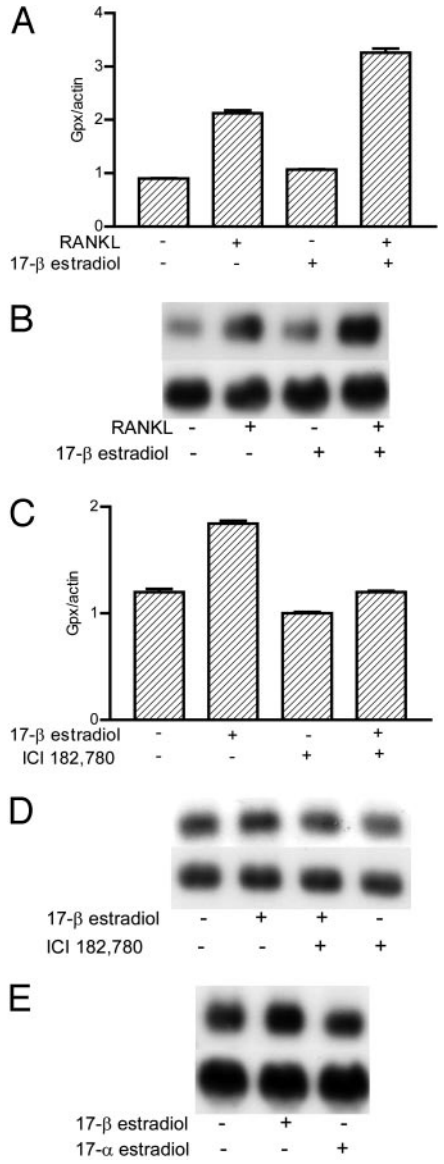

FIG. 2. Assessment of the effects of RANKL and 17β-estradiol on Gpx1 expression by murine bone marrow-derived cells. A and B, Real-time PCR assessment and Northern analysis of Gpx1 mRNA expression relative to actin in bone marrow macrophages incubated for 5 d in M-CSF with/without RANKL, treated with or without 17β-estradiol (10^{-9} M) for the last 24 h. C and D, Real-time PCR assessment and Northern analysis of Gpx1 mRNA expression relative to actin in bone marrow-derived macrophages incubated in M-CSF and RANKL for 5 d and then incubated with 17β-estradiol (10^{-9} M), ICI 182,780 (10^{-7} M), or both for the last 24 h. E, Northern analysis of bone marrow-derived osteoclastic cells treated with 17β-estradiol (10^{-9} M) or 17α-estradiol (10^{-9} M) for the last 24 h.

osteoclastic differentiation and NFκB activation suggests that modulation of hydrogen peroxide by Gpx might play a role in estrogen-deficiency bone loss. To test this possibility, we administered CAT, which has been shown to transit from the circulation (19) to ovariectomized or sham-ovariectomized mice. We found that, whereas ovariectomized mice showed a substantial reduction in bone volume, this was prevented by CAT (Fig. 6). This was associated with normalization of the ovariectomy-induced increases in bone resorption. CAT did not affect the histomorphometric indices of sham-ovariectomized bone and had no effect on the body weight of the mice. These data strongly suggest that hydrogen peroxide is the cause of estrogen deficiency bone loss. The absence of effect of CAT on the bone of sham-ovariectomized mice suggests that only when Gpx levels fall does hydrogen peroxide escape cells in sufficient quantity to influence bone cell behavior.

Discussion

We found that expression of Gpx, the major enzyme responsible for the intracellular degradation of hydrogen peroxide, was amplified in osteoclasts, compared with macrophages, and was further increased by 17β-estradiol. Stable transfection of a Gpx expression construct into RAW cells abrogated osteoclastic differentiation. Suppression of osteoclast formation was associated with suppression of NFκB-activation by RANKL and TNFα and by increased resistance to hydrogen peroxide-induced oxidation of DCF in Gpx-transfected cells. The physiological significance of these observations was supported by experiments in which we found that administration of catalase prevented the loss of bone that normally follows ovariectomy in mice.

Both estrogen, which inhibits, and RANKL, which stimulates osteoclastic differentiation, induced Gpx expression in osteoclasts. With the proviso that the expression construct increases Gpx enzyme activity by a factor of 10 in the RAW cells (data not shown), the ability of Gpx overexpression in RAW cells to suppress osteoclastic differentiation suggests that this is a mechanism through which estrogen suppresses osteoclastic differentiation and that the induction of Gpx by RANKL represents negative feedback inhibition, analogous to the induction of the osteoclastogenesis-inhibitory interferon-β by RANKL (20). It is known that osteoclasts express NADPH oxidase and generate large quantities of ROS during bone resorption (8). Therefore, induction of Gpx by RANKL might reflect ROS-induced activation of signaling cascades that lead to increased expression of the antioxidant defense proteins, which, our experiments suggest, represents a negative feedback inhibition of osteoclastic differentiation.

In addition to augmentation of signaling pathways for the induction of antioxidant defense proteins, ROS will be expected to augment other ROS-sensitive pathways in osteoclasts. In fact, osteoclasts are a prime candidate for regulation by ROS: their activity is dependent on several intracellular signals that are sensitive to ROS, including NFκB, c-Jun amino-terminal kinase, phosphatidylinositol 3-kinase, and p38 MAPK (4). Consistent with this, we found that enhanced expression of Gpx suppressed activation of NFκB, a transcription factor that is crucial for osteoclast formation and function (9, 10), in osteoclasts. Because ROS potently inhibit tyrosine phosphatases (21, 22), many phosphorylation-dependent signaling cascades are likely to be influenced by ROS in osteoclasts, thereby providing further mechanisms through which modulation of osteoclastic activity might occur.

The ability of Gpx overexpression to abrogate osteoclastic differentiation suggests that among ROS, it is specifically hydrogen peroxide that is crucial for osteoclastic differenti-

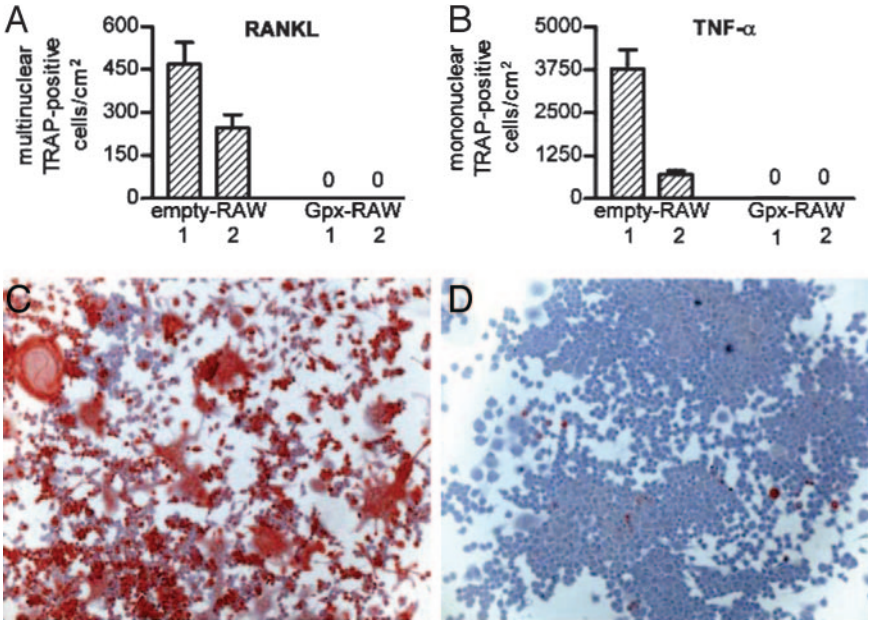

FIG. 3. Osteoclast formation is strongly inhibited in RAW cells stably transfected with Gpx1-expression vector. Two stably transfected clones of empty and Gpx-1-expressing RAW cells were incubated for 5 d on plastic coverslips in the presence of RANKL (100 ng/ml) or TNFα (100 ng/ml). A, Quantification of TRAP-positive cells in cultures of RAW cells stably transfected with Gpx1 expression vector (Gpx-RAW) or empty vector (empty-RAW) treated with 100 ng/ml RANKL. B, Quantification of TRAP-positive cells in cultures of RAW cells stably transfected with Gpx1 expression vector (Gpx-RAW) or empty vector (empty-RAW) treated with 100 ng/ml TNFα. C, Photomicrographs of empty-RAW cells (C) or Gpx-RAW cells (D) after incubation in RANKL (100 ng/ml). Results derived from six cultures per variable. Results shown as mean ± SEM.

ation. Among ROS, hydrogen peroxide has the characteristics most suited to act as both an intra- and intercellular signal because it has a relatively long half-life and is membrane permeant (23). It has moreover been shown to directly stimulate osteoclast formation and function (5, 7), and CAT suppresses osteoclastic differentiation *in vitro* (24). In fact, many cytokines and growth factors have been shown to activate cells through NADPH oxidase-mediated hydrogen peroxide production, and we showed that suppression of osteoclastic differentiation by Gpx overexpression was associated with suppression of DCF-fluorescence by exogenous hydrogen peroxide. Thus, hydrogen peroxide not only augments osteoclastic differentiation and function but also is essential for osteoclastic differentiation.

The ability of CAT to prevent osteopenia after ovariectomy establishes that hydrogen peroxide is responsible for estrogen-deficiency bone loss. The source of the hydrogen peroxide is uncertain, but the osteoclast has been shown to be a major source in bone (8). CAT did not detectably influence the bones of intact mice, suggesting that hydrogen peroxide appears in the extracellular fluid of bone increase under conditions of estrogen deficiency. We found that Gpx expression in osteoclasts is lower in the absence of estrogen so that we would anticipate a tendency for this to occur after ovariectomy.

Our finding that CAT administration prevents the bone loss caused by ovariectomy represents strong evidence that our *in vitro* findings have significance for the pathophysiology of bone. The observation that Gpx is decreased in the plasma of osteopenic patients supports the potential significance of our findings for bone pathophysiology in women (25). The effect of CAT on bone loss also has further significance. CAT, unlike hydrogen peroxide, is unable to diffuse across cell membranes. Therefore, suppression of bone loss

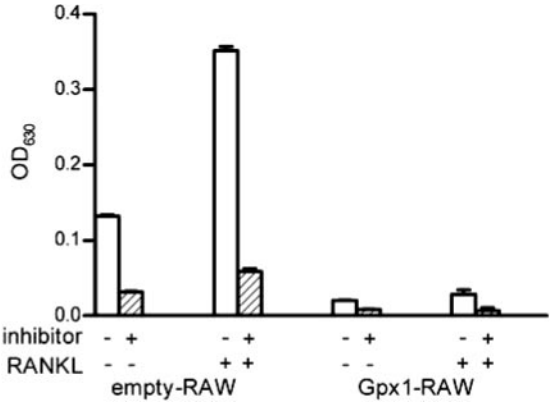

FIG. 4. Stable transfection of RAW cells with Gpx expression vector strongly suppresses NFκB activation. An increase in NFκB binding correlates with the increase in OD_{630}. Stably transfected RAW cells with either empty vector or Gpx1 expression vector were treated for 1 h with 50 ng/ml RANKL and nuclear extracts harvested. RANKL strongly activates NFκB binding in empty-RAW cells, whereas this was abolished in the Gpx-RAW cells. The competitor oligo inhibits NFκB binding showing specificity.

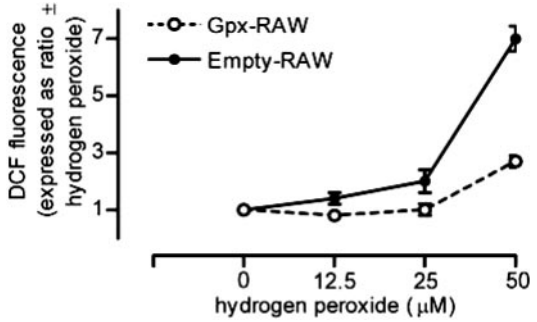

FIG. 5. Gpx-RAW cells are more able to resist oxidation of DCF caused by exogenous H_2O_2 than empty-RAW cells. RAW cells stably transfected with Gpx or empty expression vector were incubated in DCFH-DA for 15 min and then with/without hydrogen peroxide for a further 10 min. Fluorescence was then measured in a plate reader. The results are expressed as the ratio of fluorescence of cells incubated with hydrogen peroxide to that of cells incubated without hydrogen peroxide. The results are expressed as the ratio of fluorescence of DCF in the presence *vs.* the absence of H_2O_2.

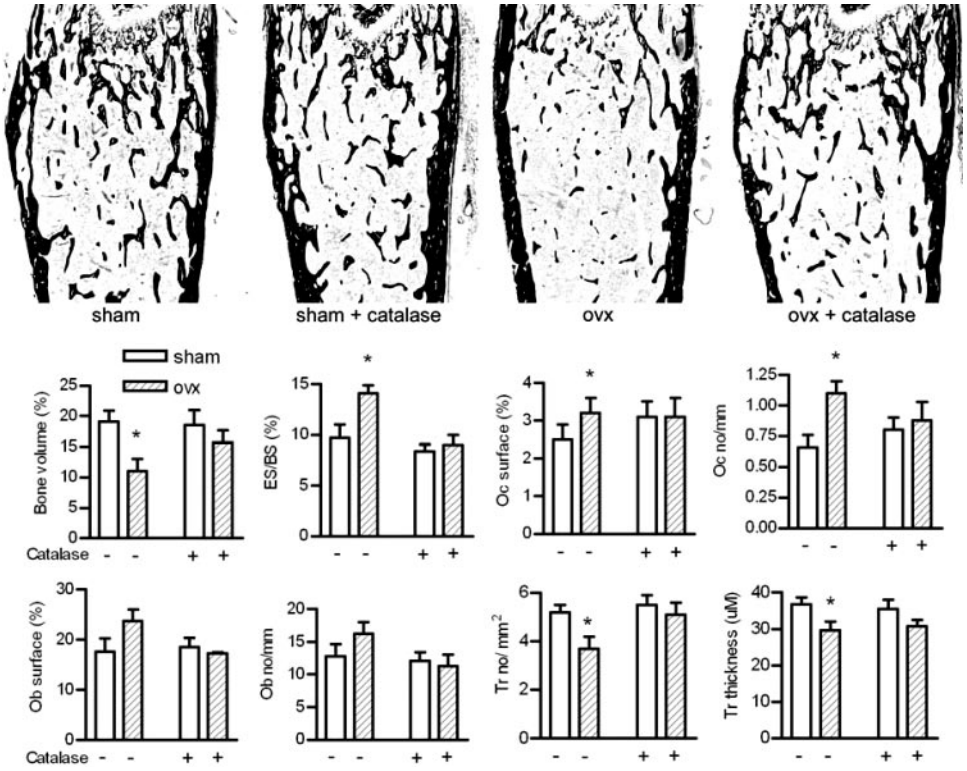

FIG. 6. Pegylated CAT inhibits the bone loss induced by ovariectomy (ovx). Groups of eight mice were ovariectomized/sham ovariectomized and injected with CAT (250 U per mouse ip) or vehicle daily for 2 wk. ES/BS, percentage of bone surface showing an eroded appearance; oc/ob surface, the percentage of bone surfaces covered by osteoclasts or osteoblasts; oc/ob no, the number of osteoclasts or osteoblasts on bone surfaces; tr no and tr thickness, the number and thickness of trabeculae. *, $P < 0.05$ *vs.* sham.

by CAT is due to degradation of hydrogen peroxide in the extracellular space. This suggests that hydrogen peroxide causes bone loss through a paracrine or autocrine action. Thus, in addition to the direct effect of hydrogen peroxide on signal cascades essential for osteoclast formation, demonstrated by the ability of Gpx overexpression to abrogate osteoclastic differentiation, hydrogen peroxide might also indirectly stimulate osteoclasts. A common consequence of the exposure of cells to hydrogen peroxide is the induction of expression cytokines such as TNFα, IL-1, and IL-6, which have been strongly implicated in estrogen-deficiency bone loss (26, 27). Recently it was shown that TNFα synergizes strongly with RANKL for osteoclast formation and activation (28, 29) and that mice lacking TNFα signaling do not lose bone after ovariectomy (27). This makes it possible that the autocrine-paracrine effects of hydrogen peroxide-induced TNFα expression in osteoclasts, osteoblasts, or other cells in the bone microenvironment might contribute to the bone loss caused by hydrogen peroxide. Similarly, hydrogen peroxide might cause bone loss by up-regulation or down-regulation of the expression by bone cells of RANKL or osteoprotegerin, the decoy receptor for RANKL, or through the induction of apoptosis in osteoblastic cells (30).

These results have important implications for bone biology and the treatment of osteoporosis. The results predict that not only the bone loss of estrogen deficiency but also that seen in other situations in which ROS have been implicated, such as in aging and inflammation, might be caused by a prolonged augmentation of ROS signaling in bone cells. Thus, ROS generated by inflammatory tissue in or adjacent to bone might cause the loss of bone that is a feature of diseases such as rheumatoid arthritis or periodontitis. Furthermore, osteoporosis has recently been noted in two mouse models of premature aging associated with oxidative damage (31, 32) in which osteopenia is presumed to be the consequence of oxidative damage. It may be that estrogen deprivation, by lowering osteoclastic thiol antioxidant levels, leads to oxidative damage and that this, rather than signal modulation, causes bone loss. Alternatively, signal modulation by the increased oxidant stress in these models of premature aging might account for the bone loss. Whichever mechanism underlies the bone loss, our results predict that osteoporosis should be prevented by therapies that increase the degradation of hydrogen peroxide in bone.

Acknowledgments

Received August 4, 2004. Accepted October 27, 2004.

Address all correspondence and requests for reprints to: Professor T. J. Chambers, Department of Cellular Pathology, St. George's Hospital Medical School, Cranmer Terrace, London SW17 0RE, United Kingdom. E-mail: tchamber@sghms.ac.uk.

This work was supported by the Wellcome Trust.

References

1. **Chambers TJ** 2000 Regulation of the differentiation and function of osteoclasts. J Pathol 192:4–13
2. **Riggs BL, Khosla S, Melton III LJ** 2002 Sex steroids and the construction and conservation of the adult skeleton. Endocr Rev 23:279–302
3. **Boyle WJ, Simonet WS, Lacey DL** 2003 Osteoclast differentiation and activation. Nature 423:337–342
4. **Dröge W** 2002 Free radicals in the physiological control of cell function. Physiol Rev 82:47–95
5. **Bax BE, Alam ASMT, Banerji B, Bax CMR, Bevis PJR, Stevens CR, Moonga BS, Blake DR, Zaidi M** 1992 Stimulation of osteoclastic bone resorption by hydrogen peroxide. Biochem Biophys Res Commun 183:1153–1158
6. **Garrett IR, Boyce BF, Oreffo ROC, Bonewald L, Poser J, Mundy GR** 1990

Oxygen-derived free radicals stimulate osteoclastic bone resorption in rodent bone *in vitro* and *in vivo*. J Clin Invest 85:632–639
7. **Lean JM, Davies JT, Fuller K, Jagger CJ, Kirstein B, Partington GA, Urry ZL, Chambers TJ** 2003 A crucial role for thiol antioxidants in estrogen-deficiency bone loss. J Clin Invest 112:915–923
8. **Steinbeck MJ, Appel Jr WH, Verhoeven AJ, Karnovsky MJ** 1994 NADPH-oxidase expression and *in situ* production of superoxide by osteoclasts actively resorbing bone. J Cell Biol 126:765–772
9. **Hall TJ, Schaueblin M, Jeker H, Fuller K, Chambers TJ** 1995 The role of reactive oxygen intermediates in osteoclastic bone resorption. Biochem Biophys Res Commun 207:280–287
10. **Franzoso G, Carlson L, Xing L, Poljak L, Shores EW, Brown KD, Leonardi A, Tran T, Boyce BF, Siebenlist U** 1997 Requirement for NF-κB in osteoclast and B-cell development. Genes Dev 11:3482–3496
11. **Schreck R, Rieber P, Baeuerle PA** 1991 Reactive oxygen intermediates as apparently widely used messengers in the activation of the NF-κB transcription factor and HIV-1. EMBO J 10:2247–2258
12. **Baeuerle PA, Baltimore D** 1996 NF-κB: ten years after. Cell 87:13–20
13. **Piette J, Piret B, Bonizzi G, Schoonbroodt S, Merville MP, Legrand-Poels S, Bours V** 1997 Multiple redox regulation in NF-κB transcription factor activation. Biol Chem 378:1237–1245
14. **Wani MR, Fuller K, Kim NS, Choi Y, Chambers T** 1999 Prostaglandin E_2 cooperates with TRANCE in osteoclast induction from hemopoietic precursors: synergistic activation of differentiation, cell spreading, and fusion. Endocrinology 140:1927–1935
15. **Lean JM, Murphy C, Fuller K, Chambers TJ** 2002 CCL9/MIP-1γ and its receptor CCR1 are the major chemokine ligand/receptor species expressed by osteoclasts. J Cell Biochem 87:386–393
16. **Lean JM, Matsuo K, Fox SW, Fuller K, Gibson FM, Draycott G, Wani MR, Bayley KE, Wong BR, Choi Y, Wagner EF, Chambers TJ** 2000 Osteoclast lineage commitment of bone marrow precursors through expression of membrane-bound TRANCE. Bone 27:29–40
17. **Negre-Salvayre A, Auge N, Duval C, Robbesyn F, Thiers JC, Nazzal D, Benoist H, Salvayre R** 2002 Detection of intracellular reactive oxygen species in cultured cells using fluorescent probes. Methods Enzymol 352:62–71
18. **Chow J, Tobias JH, Colston KW, Chambers TJ** 1992 Estrogen maintains trabecular bone volume in rats not only by suppression of bone resorption but also by stimulation of bone formation. J Clin Invest 89:74–78
19. **Winn LM, Wells PG** 1999 Maternal administration of superoxide dismutase and catalase in phenytoin teratogenicity. Free Radic Biol Med 26:266–274
20. **Takayanagi H, Kim S, Matsuo K, Suzuki H, Suzuki T, Sato K, Yokochi T, Oda H, Nakamura K, Ida N, Wagner EF, Taniguchi T** 2002 RANKL maintains bone homeostasis through c-Fos dependent induction of interferon-β. Nature 416:744–749
21. **Caselli A, Marzocchini R, Camici G, Manao G, Moneti G, Pieraccini G** 1998 The inactivation mechanism of low molecular weight phosphotyrosine-protein phosphatase by H2O2. J Biol Chem 273:32554–32560
22. **Xu D, Rovira II, Finkel T** 2002 Oxidants painting the cysteine chapel: redox regulation of PTPs. Dev Cell 2:251–252
23. **Reth M** 2002 Hydrogen peroxide as second messenger in lymphocyte activation. Nature 3:1129–1133
24. **Suda N, Morita I, Kuroda T, Murota S** 1993 Participation of oxidative stress in the process of osteoclastic differentiation. Biochim Biophys Acta 1157:318–323
25. **Maggio D, Barabani M, Pierandrei M, Polidori MC, Catani M, Mecocci P, Senin U, Pacifici R, Cherubini A** 2003 Marked decrease in plasma antioxidants in aged osteoporotic women: results of a cross-sectional study. J Clin Endocrinol Metab 88:1523–1527
26. **Kitazawa R, Kimble RB, Vannice JL, Kung VT, Pacifici R** 1994 Interleukin-1 receptor antagonist and tumor necrosis factor binding protein decrease osteoclast formation and bone resorption in ovariectomized mice. J Clin Invest 94:2397–2406
27. **Roggia C, Gao Y, Cenci S, Weitzmann MN, Toraldo G, Isaia G, Pacifici R** 2001 Up-regulation of TNF-producing T cells in the bone marrow: a key mechanism by which estrogen deficiency induces bone loss *in vivo*. Proc Natl Acad Sci USA 98:13960–13965
28. **Fuller K, Murphy C, Kirstein B, Fox SW, Chambers TJ** 2002 TNFα potently activates osteoclasts, through a direct action independent of and strongly synergistic with RANKL. Endocrinology 143:1108–1118
29. **Lam J, Takeshita S, Barker JE, Kanagawa O, Ross FP, Teitelbaum SL** 2000 TNF-α induces osteoclastogenesis by direct stimulation of macrophages exposed to permissive levels of RANK ligand. J Clin Invest 106:1481–1488
30. **Kousteni S, Chen JR, Bellido T, Han L, Ali AA, O'Brien CA, Plotkin LI, Fu Q, Mancino AT, Wen Y, Vertino AM, Powers CC, Stewart SA, Ebert R, Parfitt AM, Weinstein RS, Jilka RL, Manolagas SC** 2002 Reversal of bone loss in mice by nongenotropic signaling of sex steroids. Science 298:843–846
31. **Tyner SD, Venkatachalam S, Choi J, Jones SM, Ghebranious N, Igelmann H, Lu X, Soron G, Cooper B, Brayton C, Hee Park S, Thompson T, Karsenty G, Bradley A, Donehower LA** 2002 p53 mutant mice that display early ageing-associated phenotypes. Nature 415:45–53
32. **de Boer J, Andressoo JO, de Wit J, Huijmans J, Beems RB, van Steeg H, Weeda G** 2002 Premature aging in mice deficient in DNA repair and transcription. Science 296:1276–1279

***Endocrinology* is published monthly by The Endocrine Society (http://www.endo-society.org), the foremost professional society serving the endocrine community.**